

Generation and Mixing of Subfemtoliter Aqueous Droplets On Demand

Jianyong Tang,[†] Ana M. Jofre,[†] Rani B. Kishore,[†] Joseph E. Reiner,[‡] Mark E. Greene,[†] Geoffrey M. Lowman,[†] John S. Denker,[†] Christina C. C. Willis,[†] Kristian Helmerston,[†] and Lori S. Goldner^{*†§}

Physics Laboratory and Electronics and Electrical Engineering Laboratory, National Institute of Standards and Technology, Gaithersburg, Maryland 20899 and Physics Department, University of Massachusetts, Amherst, Massachusetts 01003

We describe a novel method of generating monodisperse subfemtoliter aqueous droplets on demand by means of piezoelectric injection. Droplets with volumes down to 200 aL are generated by this technique. The droplets are injected into a low refractive index perfluorocarbon so that they can be optically trapped. We demonstrate the use of optical tweezers to manipulate and mix droplets. For example, using optical tweezers we bring two droplets, one containing a calcium sensitive dye and the other calcium chloride, into contact. The droplets coalesce with a resulting reaction time of about 1 ms. The monodispersity, manipulability, repeatability, small size, and fast mixing afforded by this system offer many opportunities for nanochemistry and observation of chemical reactions on a molecule-by-molecule basis.

The controlled and confining environment afforded by various molecular nanocontainers and microemulsions has long been utilized by chemists. In organic reactions, thermodynamically stable microemulsions are commonly used to overcome the problem of reactant incompatibility.¹ Molecular and macromolecular cages, micellar containers, vesicles, polymersomes, and polyelectrolyte cages have been used to confine and catalyze reactions that otherwise would be prohibitively slow.² Small emulsion droplets have found particular application in nanoparticle synthesis^{3,4} and have also been used in the study of enzymatic reactions, including single enzyme kinetics,^{5–7} and in molecular evolution.^{8–10} Polymerase chain reaction (PCR) performed at the

single molecule level in emulsion droplets^{9,11,12} has found numerous applications.^{10,13–18} The many applications of droplet-based bioreactors has engendered the development of microfluidic techniques to form droplets^{19–26} and integrated devices to react and probe their contents.^{27–30}

* Corresponding author. E-mail: lgoldner@physics.umass.edu.

[†] Physics Laboratory, National Institute of Standards and Technology.

[‡] Electronics and Electrical Engineering Laboratory, National Institute of Standards and Technology.

[§] University of Massachusetts.

- (1) Holmberg, K. *Eur. J. Org. Chem.* **2007**, 731–742.
- (2) Vriezema, D. M.; Aragones, M. C.; Elemans, J.; Cornelissen, J.; Rowan, A. E.; Nolte, R. J. M. *Chem. Rev.* **2005**, *105*, 1445–1489.
- (3) Landfester, K. *Ann. Rev. Mater. Res.* **2006**, *36*, 231–279.
- (4) Shchukin, D. G.; Sukhorukov, G. B. *Adv. Mater.* **2004**, *16*, 671–682.
- (5) Rotman, B. *Proc. Natl. Acad. Sci. U.S.A.* **1961**, *47*, 1981.
- (6) Lee, A. I.; Brody, J. P. *Biophys. J.* **2005**, *88*, 4303–4311.
- (7) Hase, M.; Yamada, A.; Hamada, T.; Baigl, D.; Yoshikawa, K. *Langmuir* **2007**, *23*, 348–352.
- (8) Tawfik, D. S.; Griffiths, A. D. *Nat. Biotechnol.* **1998**, *16*, 652–656.
- (9) Ghadessy, F. J.; Ong, J. L.; Holliger, P. *Proc. Natl. Acad. Sci. U.S.A.* **2001**, *98*, 4552–4557.
- (10) Griffiths, A. D.; Tawfik, D. S. *Trends Biotechnol.* **2006**, *24*, 395–402.

- (11) Nakano, M.; Komatsu, J.; Matsuura, S.; Takashima, K.; Katsura, S.; Mizuno, A. *J. Biotechnol.* **2003**, *102*, 117–124.
- (12) Musyanovych, A.; Mailander, V.; Landfester, K. *Biomacromolecules* **2005**, *6*, 1824–1828.
- (13) Dressman, D.; Yan, H.; Traverso, G.; Kinzler, K. W.; Vogelstein, B. *Proc. Natl. Acad. Sci. U.S.A.* **2003**, *100*, 8817–8822.
- (14) Nakano, M.; Nakai, N.; Kurita, H.; Komatsu, J.; Takashima, K.; Katsura, S.; Mizuno, A. *J. Biosci. Bioeng.* **2005**, *99*, 293–295.
- (15) Wetmur, J. G.; Kumar, M.; Zhang, L.; Palomeque, C.; Wallenstein, S.; Chen, J. *Nucleic Acids Res.* **2005**, *33*, 2615–2619.
- (16) Shendure, J.; Porreca, G. J.; Reppas, N. B.; Lin, X. X.; McCutcheon, J. P.; Rosenbaum, A. M.; Wang, M. D.; Zhang, K.; Mitra, R. D.; Church, G. M. *Science* **2005**, *309*, 1728–1732.
- (17) Margulies, M.; Egholm, M.; Altman, W. E.; Attiya, S.; Bader, J. S.; Bemben, L. A.; Berka, J.; Braverman, M. S.; Chen, Y. J.; Chen, Z. T.; Dewell, S. B.; Du, L.; Fierro, J. M.; Gomes, X. V.; Godwin, B. C.; He, W.; Helgesen, S.; Ho, C. H.; Irzyk, G. P.; Jando, S. C.; Alenquer, M. L. L.; Jarvie, T. P.; Jirage, K. B.; Kim, J. B.; Knight, J. R.; Lanza, J. R.; Leamon, J. H.; Lefkowitz, S. M.; Lei, M.; Li, J.; Lohman, K. L.; Lu, H.; Makhijani, V. B.; McDade, K. E.; McKenna, M. P.; Myers, E. W.; Nickerson, E.; Nobile, J. R.; Plant, R.; Puc, B. P.; Ronan, M. T.; Roth, G. T.; Sarkis, G. J.; Simons, J. F.; Simpson, J. W.; Srinivasan, M.; Tartaro, K. R.; Tomasz, A.; Vogt, K. A.; Volkmer, G. A.; Wang, S. H.; Wang, Y.; Weiner, M. P.; Yu, P. G.; Begley, R. F.; Rothberg, J. M. *Nature* **2005**, *437*, 376–380.
- (18) Kojima, T.; Takei, Y.; Ohtsuka, M.; Kawarasaki, Y.; Yamane, T.; Nakano, H. *Nucleic Acids Res.* **2005**, *33*, 9.
- (19) Thorsen, T.; Roberts, R. W.; Arnold, F. H.; Quake, S. R. *Phys. Rev. Lett.* **2001**, *86*, 4163–4166.
- (20) Song, H.; Tice, J. D.; Ismagilov, R. F. *Angew. Chem., Int. Ed.* **2003**, *42*, 768–772.
- (21) Anna, S. L.; Bontoux, N.; Stone, H. A. *Appl. Phys. Lett.* **2003**, *82*, 364–366.
- (22) Link, D. R.; Anna, S. L.; Weitz, D. A.; Stone, H. A. *Phys. Rev. Lett.* **2004**, *92*.
- (23) He, M. Y.; Kuo, J. S.; Chiu, D. T. *Appl. Phys. Lett.* **2005**, *87*, 031916.
- (24) Garstecki, P.; Fuerstman, M. J.; Stone, H. A.; Whitesides, G. M. *Lab Chip* **2006**, *6*, 437–446.
- (25) Lorenz, R. M.; Edgar, J. S.; Jeffries, G. D. M.; Chiu, D. T. *Anal. Chem.* **2006**, *78*, 6433–6439.
- (26) Christopher, G. F.; Anna, S. L. *J. Phys., D: Appl. Phys.* **2007**, *40*, R319–R336.
- (27) Link, D. R.; Grasland-Mongrain, E.; Duri, A.; Sarrazin, F.; Cheng, Z. D.; Cristobal, G.; Marquez, M.; Weitz, D. A. *Angew. Chem., Int. Ed.* **2006**, *45*, 2556–2560.
- (28) Ahn, K.; Kerbage, C.; Hunt, T. P.; Westervelt, R. M.; Link, D. R.; Weitz, D. A. *Appl. Phys. Lett.* **2006**, *88*, 3.
- (29) Courtois, F.; Olguin, L. F.; Whyte, G.; Bratton, D.; Huck, W. T. S.; Abell, C.; Hollfelder, F. *ChemBioChem* **2008**, *9*, 439–446.
- (30) Beer, N. R.; Hindson, B. J.; Wheeler, E. K.; Hall, S. B.; Rose, K. A.; Kennedy, I. M.; Colston, B. W. *Anal. Chem.* **2007**, *79*, 8471–8475.

In addition to the advantages of simple confinement, droplet nanoreactors can be individually manipulated and mixed allowing the study of fast reaction dynamics. Intrinsically fast diffusional mixing in nanoscopic droplets enables control and determination of mixing time with an accuracy of a few milliseconds. Confinement also allows reaction dynamics to be studied for extended time scales, limited only by the measurement technique rather than by diffusion or flow rate.^{31,32} This can be particularly useful in the study of reaction dynamics at the single molecule scale, where confinement permits both fast mixing and containment of the reactants in a detection volume.

For accurate and repeatable measurements, droplet-based nanoreactors must be reproducible in size and composition, and be easily manipulated and mixed. With the use of microfluidics or with the technique we describe here, droplet size and composition are easily controlled. The surfaces of droplets can be tailored with the addition of amphiphiles, and depending on the choice of amphiphile, droplets coalesce on contact or remain stable against coalescence.

For improved sensitivity, efficiency, and waste reduction, small droplet sizes are desirable. To study reaction on a molecule-by-molecule basis, droplets in the range from 0.1 to 100 fL work well. They are small enough to contain only one biomolecule at plausible physiological concentrations, yet are large enough to be optically trapped and manipulated. With dependence on the choice or absence of surfactant, interactions between the droplet boundary and confined molecules can be minimized so that molecules diffuse freely in the droplet,³³ an advantage over other methods of manipulating or confining single molecules that require the molecules to be attached to a surface or bead.

Commonly called nano- or mini-emulsions, metastable suspensions of water-in-oil droplets less than a micrometer in size, can be generated by a variety of methods,^{34,35} often involving extreme shear generated by ultrasound or high-pressure homogenizers. Droplets as small as a few tens of nanometers in diameter can be generated this way, but the size and size distribution are difficult to control, and the agitation process is damaging to some biomolecules.¹²

Droplets with volume between 1 fL and 1 nL are now commonly produced in continuous streams using microfluidic techniques.^{19–24} T-shaped channels^{19,20,22,24} or flow focusing techniques²¹ provide good control of droplet size and size distribution for larger emulsion droplets confined in a planar geometry. Microcapillary-based devices produce similarly sized monodisperse droplets continuously in a true three-dimensional geometry.^{36,37} Monodisperse emulsions with picoliter droplets

have also been formed using microchannel plates.³⁸ While droplet formation on demand is not yet common in microfluidic devices, it has recently been demonstrated for larger droplets using a piezo-actuated polydimethylsiloxane device.³⁹ A commercially available microinjector has also been used to produce femtoliter and larger droplets on demand in a microchannel device.²⁵

Here we describe and characterize a piezo-electrically driven inertial injector that generates monodisperse subfemtoliter droplets on demand. We measure the droplet size using a stoichiometric technique and demonstrate fast mixing using the change in fluorescence of a calcium sensing dye upon mixing with calcium. Based on a sharpened microcapillary tube, the injector is piezoelectrically driven to permit formation of small and monodisperse droplets. Similar in some ways to two previous devices,^{40,41} this device differs in the details of construction and the mode of operation. Droplets produced have volumes tunable between 200 aL and 10 fL, smaller than is usual for microfluidics. Control and mixing is achieved through optical manipulation of the droplets.⁴²

We have previously demonstrated the use of this injector and showed that enhanced green fluorescent protein (EGFP) could be confined in injected droplets with an efficiency at or near 100%.³³ Time-resolved fluorescence polarization anisotropy measurement demonstrated the rotational diffusion of EGFP in free solution and in the droplets is indistinguishable. Single molecule detection inside of optically trapped droplets has been separately demonstrated.^{33,42}

Perfluorinated oils, which have refractive index ($n = 1.28–1.30$) lower than that of water ($n = 1.33$), are used for the continuous phase in this work. This index difference makes it possible to use optical tweezers^{43,44} to trap and manipulate the aqueous droplets.⁴² Other optical techniques can be used to manipulate⁴⁵ and even trap droplets in high refractive-index oil,^{46,47} but it is convenient to use conventional optical tweezers.^{43,44}

METHODS

Chemicals. SigmaCote, calcium chloride, Triton X-100, and PEG methyl ether are from Sigma-Aldrich. Perfluorotriamylamine (FC-70) is from 3 M Corp and Fluo-3 pentapotassium salt (F-3715) is from Molecular Probes. All solutions are filtered through 0.2 μm syringe filters.

(31) White, S. S.; Balasubramanian, S.; Klenerman, D.; Ying, L. M. *Angew. Chem., Int. Ed.* **2006**, *45*, 7540–7543.
(32) Lipman, E. A.; Schuler, B.; Bakajin, O.; Eaton, W. A. *Science* **2003**, *301*, 1233–1235.
(33) Tang, J.; Jofre, A. M.; Lowman, G. M.; Kishore, R. B.; Reiner, J. E.; Helmersson, K.; Goldner, L. S.; Greene, M. E. *Langmuir* **2008**, *24*, 4975–4978.
(34) Mason, T. G.; Wilking, J. N.; Meleson, K.; Chang, C. B.; Graves, S. M. *J. Phys.: Condens. Matter* **2006**, *18*, R635–R666.
(35) Solans, C.; Izquierdo, P.; Nolla, J.; Azemar, N.; Garcia-Celma, M. *J. Curr. Opin. Colloid Interface Sci.* **2005**, *10*, 102–110.
(36) Umbanhowar, P. B.; Prasad, V.; Weitz, D. A. *Langmuir* **2000**, *16*, 347–351.
(37) Utada, A. S.; Lorenceau, E.; Link, D. R.; Kaplan, P. D.; Stone, H. A.; Weitz, D. A. *Science* **2005**, *308*, 537–541.

(38) Sugiura, S.; Nakajima, M.; Iwamoto, S.; Seki, M. *Langmuir* **2001**, *17*, 5562–5566.
(39) Xu, J.; Attinger, D. *J. Micromech. Microeng.* **2008**, *18*.
(40) Lee, C. H.; Lal, A. *IEEE Trans. Ultrason. Ferroelectr. Freq. Control* **2004**, *51*, 1514–1522.
(41) Zhang, W. Y.; Hou, L. Y.; Mu, L. L.; Zhu, L. In *Microfluidics, BioMEMS, and Medical Microsystems II*. Proceedings of the Society of Photo-optical Instrumentation Engineers (SPIE); Woias, P., Papautsky, I., Eds.; 2004; Vol. 5345, pp 220–229.
(42) Reiner, J. E.; Crawford, A. M.; Kishore, R. B.; Goldner, L. S.; Helmersson, K.; Gilson, M. K. *Appl. Phys. Lett.* **2006**, *89*, 013904.
(43) Ashkin, A. *Proc. Natl. Acad. Sci. U.S.A.* **1997**, *94*, 4853–4860.
(44) Svoboda, K.; Block, S. M. *Annu. Rev. Biophys. Biomol. Struct.* **1994**, *23*, 247–285.
(45) Katsura, S.; Yamaguchi, A.; Inami, H.; Matsuura, S.; Hirano, K.; Mizuno, A. *Electrophoresis* **2001**, *22*, 289–293.
(46) Sasaki, K.; Koshioka, M.; Misawa, H.; Kitamura, N.; Masuhara, H. *Appl. Phys. Lett.* **1992**, *60*, 807–809.
(47) Lorenz, R. M.; Edgar, J. S.; Jeffries, G. D. M.; Zhao, Y. Q.; McGloin, D.; Chiu, D. T. *Anal. Chem.* **2007**, *79*, 224–228.

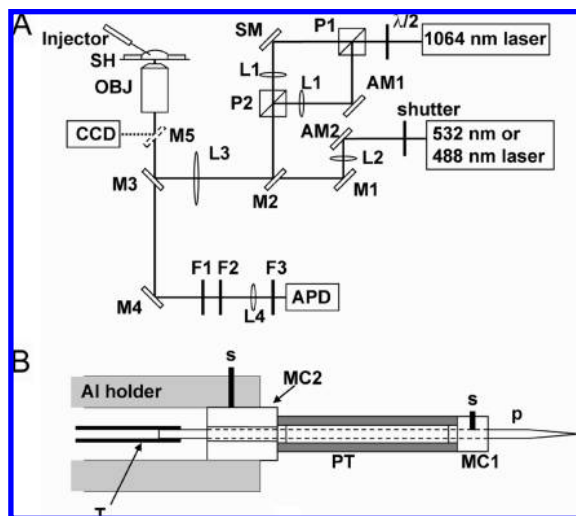


Figure 1. (A) Experimental setup: M1, M2, M3–M5, mirrors; SM, AM1, and AM2 are mirrors used for beam steering or adjustment; M2 is an IR mirror that passes visible light. M3 is a dichroic mirror in the microscope slider. M5 is a flip mirror or prism internal to the microscope used to divert light to the camera (charge-coupled device, CCD). L1: lenses that along with L3 image SM and AM1 to the back focal plane of the objective. AM2 is imaged onto the back focal plane of the objective by L2 and L3. P1 and P2 are polarizing beamsplitters. F1 is an IR blocking filter or filters; F2 is a 532 or 488 nm notch filter; F3 is a fluorescence bandpass filter. SH is the sample holder; OBJ is a 100 \times oil immersion objective lens with NA 1.30. APD is a single-photon-counting avalanche photodiode detector. (B) Schematic representation of the piezoelectric driven inertial injector showing the set screws (s) that hold the glass micropipet (p) in the front macor end-cap (MC1) and the back macor end-cap (MC2) in the Al holder. PT is the piezoelectric tube.

Optical Apparatus. The experimental setup for optical manipulation and fluorescence detection is described in Figure 1A and in the Supporting Information.

Droplet Injector. The droplet injector is shown in Figure 1B. A piezoelectric tube (EBL Products Inc. type EBL 2, 3.175 mm o.d. \times 0.508 mm wall \times 25.4 mm length) with single inner and outer nickel electrodes is fitted with Macor end-caps MC1 and MC2. MC1 holds a sharpened microcapillary tube (also called micropipet) in place with a set screw, and MC2 serves as a structural base for the injector. MC2 is mounted onto an aluminum (Al) holder that is fixed on a three-dimensional translation stage with micrometer adjusters. The sharpened end of the micropipet protrudes from the front of the injector, and the microcapillary end extends out the back of MC2.

Samples are loaded into the unsharpened end of the micropipet before it is sealed to a section of Tygon microbore poly(vinyl chloride) (PVC) tubing, (i.d. 1.0 mm, o.d. 1.8 mm) using cyanoacrylate superglue (Loctite) and accelerator (Loctite 7113). After the glue dries (less than 5 s with accelerator), the loaded micropipet and piezo assembly is mounted in the Al holder and the micropipet tip is immersed into fluorocarbon FC-70 medium which sits in a sample well on the microscope stage. A backing pressure is applied from a microinjector pump (FemtoJet 5247, Eppendorf North America Inc.) to drive the sample plug to the micropipet tip. The backing pressure is adjusted so that a meniscus of sample forms near the end of the micropipet tip. To inject a nanodroplet into the FC-70, the piezoelectric tube is driven with a single cycle of a sawtooth waveform. The waveform is

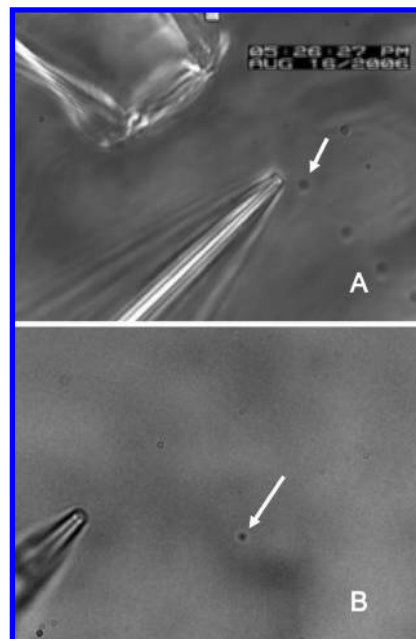


Figure 2. Nanodroplet generation and trapping. (A) Multiple nanodroplets from the injector in a flow field from the larger microcapillary. This image is taken with a 100 \times /1.30 objective and the field of view is 68 μ m by 51 μ m. The corresponding video is the first movie in the Supporting Information. (B) Droplet generation and trapping. The objective lens and field of view are the same as in part A. In both images, the white arrows indicate the location of injected aqueous droplets.

generated by an HP function generator (model 33120A, 8 ms risetime typical with fall time <100 ns) and amplified using a Krohn-Hite amplifier (model 7500, 200 V peak, 75 W, 1 MHz bandwidth). Each cycle of the sawtooth waveform causes a slow extension (over 8 ms) and quick retraction of the micropipet tip. A droplet is injected into the FC-70 with each retraction. The pipet tip is silanized to make it hydrophobic, which is necessary to ensure detachment of the droplet from the glass (see the Supporting Information). The retraction force is limited by the bandwidth of the amplifier (1 MHz) and the electrical-mechanical resonances of the device. Preparation of the glass micropipet is described in the Supporting Information.

RESULTS AND ANALYSIS

Droplet Generation. Droplet injection and trapping is demonstrated in Figure 2. In Figure 2A and the first movie in the Supporting Information, uniform droplets are generated from the injector tip at a rate of 2 per second. A gravity-driven flow from a larger microcapillary tube (upper left) drags the droplets down and to the right. In Figure 2B a single droplet is immobilized in an optical trap (white arrow) after injection.

The second movie in the Supporting Information shows a video of tip motion and droplet formation taken at 16 000 frames per second. From this video it is apparent that the droplet is fully formed, and the tip fully retracted, by the third frame (190 μ s) after tip retraction initiates. Droplets are formed with zero velocity, suggesting that the primary mechanism for droplet formation is the inertia of the aqueous buffer as the tip retracts quickly around it. Droplets are apparently formed when the forces due to tip retraction are great enough to overcome viscous and surface

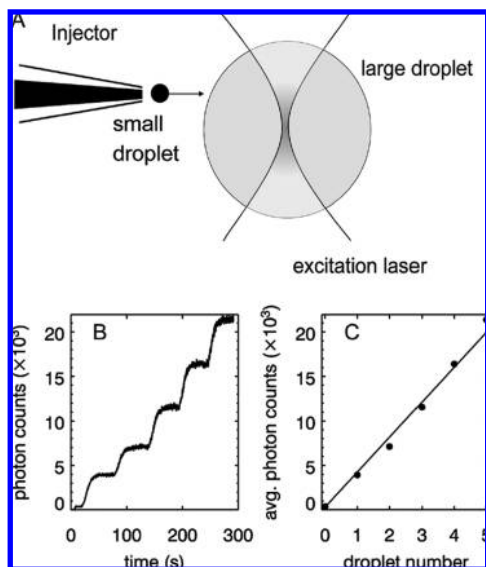


Figure 3. Stoichiometric measurement of droplet volume: (A) Schematic diagram of the experiment. (B) Plot of fluorescence intensity (photon counts in 100 ms) vs time as a series of injected droplets (with high concentration of dye solution) are mixed one by one with a larger droplet (with low concentration of dye solution). Fluorescence is measured from a fixed position near the center of the large droplet. The ratio of the dye concentrations in the small droplet to that of the large droplet is 10^6 . (C) Plot of average photon counts vs droplet number on each plateau in part B. Here the backing pressure was 700 hPa, and the peak voltage of the amplifier is -160 V, corresponding to the \bullet in Figure 4A.

forces holding the sample in the micropipet. For a fixed choice of buffer, continuous phase, and surfactant (if any), this would suggest that the droplet size will depend primarily upon the micropipet tip diameter and the details of tip retraction.

Since the droplet sizes are close to the diffraction limit of our optics, the droplet size was measured using a stoichiometric approach. A very large droplet containing a low concentration (16 nmol/L, 0.12 μ mol/L, or 0.16 μ mol/L) of sulforhodamine B was created at the end of a micropipet. This large droplet was detached from the micropipet tip but remained stationary on the side of the micropipet, which like the injector tip had a hydrophobic coating. A small droplet containing a high concentration (10^5 – 10^6 times greater than that of the large droplet) of the same dye was then generated by the injector and coalesced with the large droplet (Figure 3A). The fluorescence at the center of the large droplet is monitored with the confocal microscope during coalescence. Fluorescence increases in a stepwise fashion with each small droplet added (Figure 3B). A dilution factor can be determined from the change in fluorescence, and the diameter of the small droplets can be calculated from the dilution factor and the diameter of the large droplet. The large droplet diameter can be measured by image analysis. If the concentration of the dye in the large droplet (before adding small droplet) is $C(0)$, after adding N identical small droplets, the concentration will be $C(N)$,

$$C(N) = C(0) + \frac{r_s^3 C_s}{r_1^3} N \quad (1)$$

where r_s is the radius of the small droplet, r_1 is the radius of the large droplet, and C_s is the concentration of dye in the small

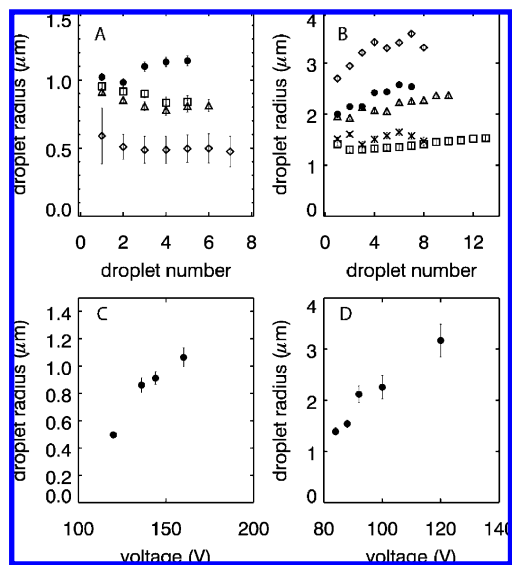


Figure 4. Droplet size measurement results: (A, B) droplet size vs injected droplet number for a small tip (A) and a large tip (B) at different amplifier voltages. The error bars in part B are smaller than or about the same size as the symbols. Legend in part A: \diamond , -120 V; Δ , -136 V; \square , -144 V; \bullet , -160 V. Legend in part B: \square , -84 V; \times , -88 V; Δ , -92 V; \bullet , -100 V; \diamond , -120 V. (C, D) Average droplet size dependence on amplifier voltage with a distribution deviation from the data sets in parts A and B, respectively.

droplet. This equation will be valid when the large droplet is sufficiently large, and N sufficiently small, that the addition of small droplets does not substantially change the volume of the large droplet. If the excitation laser maintains constant power and is focused at the same location within the large droplet, then the fluorescence intensity $I(N)$ at the detector is proportional to $C(N)$ and we can write

$$I(N) = I(0) \left(1 + \frac{r_s^3 C_s}{r_1^3 C(0)} N \right) \quad (2)$$

where $I(0) \equiv KC(0)$ and K is the proportionality constant. In a plot of $I(N)$ vs N , the small droplet size can be calculated from the slope and intercept of a fitted line, and knowledge of $C_s/C(0)$ and r_1^3 .

Figure 3B shows the stepwise intensity vs time during the course of a droplet size measurement. For each plateau we determine $I(N)$, the average fluorescence intensity on the plateau after the N th droplet. Figure 3C shows the plot of $I(N)$ vs N for a measurement with $C_s = 16$ mmol/L, $C(0) = 16$ nmol/L, and $r_1 = 96.0$ μ m. The backing pressure was 700 hPa, and the peak driving voltage was -160 V. From eq 2, we find an average small droplet radius $r_s = 2.22 \pm 0.07$ μ m or volume 46.1 ± 4.2 fL. The uncertainties are determined from the weighted least-squares fit to the data, and the fitting weights are determined by the uncertainty in the average photon count. The uncertainty in the average photon count is smaller than the deviation from the fit (χ^2 per degree of freedom is 32), and the error bars on the data in Figure 3C are smaller than the plotting symbols. The deviation from the fit therefore represents dispersion in the droplet size rather than uncertainty in the measurement technique.

The droplet size depends on the details of the tip aperture and the applied voltage at the piezoelectric. To investigate these

dependencies as well as the monodispersity of the injected droplets, we measured droplet size as a function of drive voltage amplitude for two different tips, one with a small aperture (Figure 4A, C, aperture diameter $\approx 0.5 \mu\text{m}$) and one with a large aperture (Figure 4B, D, aperture diameter $\approx 2 \mu\text{m}$). The backing pressure on the small tip was 700 hPa and on the large tip was 190 hPa. Here we make no assumption about monodispersity and simply calculate the radius of each droplet from the change in fluorescence from the large drop after adding each small drop. The error bars shown in Figure 4A,B represent the uncertainty in the individual measurements, whereas the error bars in Figure 4C,D represent the weighted average variance for all the data at a given voltage. For reference, note that droplets with radius $0.5 \mu\text{m}$ have a volume of 0.52 fL .

Figure 4 demonstrates that droplet size can be controlled by varying the peak voltage of the sawtooth driving the piezoelectric. As expected, larger tips produce larger droplets. For a given tip, larger voltages produce larger droplets. Smaller tips produce smaller droplets but require higher voltage, corresponding to higher force, to dislodge droplets. Maximum voltage is limited by the amplifier that drives our piezoelectric injector to about 200 V, although piezoelectric breakdown is a bit higher than that. This gives us the practical limit of this technique; for tips with apertures significantly smaller than used here, droplets cannot be dislodged at all. Figure 4 also shows that smaller droplets, produced at lower voltage, tend to have less dispersion in size, although for the smallest droplets the size distribution is obscured by measurement uncertainty.

The smallest droplets measured have $r_s = 368 \pm 9 \text{ nm}$ or a volume of $208 \pm 16 \text{ aL}$. For this measurement, a smaller tip was used and $C_s = 12 \text{ mmol/L}$, $C(0) = 0.12 \mu\text{mol/L}$, and $r_1 = 70 \mu\text{m}$. The backing pressure was nominally 700 hPa, and the peak voltage was near the maximum of the amplifier, 200 V. In this measurement, only the average fluorescence in the center of the large droplet after the injection of each of four small droplets was recorded. The uncertainty (weighted standard deviation of the mean) is therefore obtained assuming Poisson noise on the fluorescence measurement. While droplets this small are common in mini- or nanoemulsions, the generation and measurement of such small and monodisperse droplets on demand has not, to our knowledge, been reported elsewhere.

Droplet Mixing. With the dual trap setup shown in Figure 1A and discussed in the Supporting Information, the mixing time for two droplets was explored using a diffusion-limited reaction of calcium-sensitive dye Fluo-3 with calcium chloride (Figure 5). The injector was loaded with 100 mmol/L calcium chloride solution. The sample well was filled with a suspension of emulsified droplets containing a solution of $100 \mu\text{mol/L}$ Fluo-3 and 10 mmol/L ethylene glycol tetraacetic acid (EGTA) in FC-70. EGTA was used to remove background calcium ions before mixing. The emulsified droplet density was very low so that the probability of two or more droplets interacting was negligible. Calcium chloride containing droplets were injected into the FC-70 and then maneuvered (using the microscope stage) into one optical trap (trap 1). The microscope stage was then slowly translated to find and trap a droplet containing Fluo-3 in the second trap (trap 2), which was located in the confocal detection region.

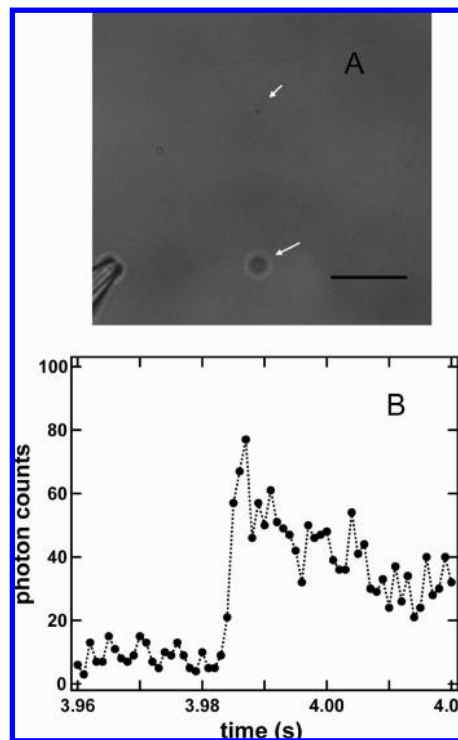


Figure 5. (A) Image of two droplets in traps before mixing, taken with a $\text{NA} = 1.3$ oil immersion lens. Scale bar is $10 \mu\text{m}$. The lower arrow indicates the injected droplet containing 100 mM calcium chloride with 0.1% Triton X-100 in HEPES buffer. The upper arrow indicates the droplet from the emulsion containing 1.0 mM Fluo-3 with 10 mM EGTA and 0.1% Triton X-100 in MOPS buffer. (B) The fluorescence (photon counts in 1 ms bins) vs time from the droplet containing Fluo-3 before, during, and after mixing with a CaCl_2 containing droplet.

Once both droplets were trapped, the bright field illumination was turned off and optical trap 1 was moved toward optical trap 2. Before the trapped droplets came in contact, the excitation laser was turned on. Fluorescence was detected from trap 2 before, during, and after droplet fusion. Data are shown in Figure 5B. There is a rapid increase in fluorescence after a droplet containing Fluo-3 was coalesced with a droplet containing calcium chloride, with the majority of the increase occurring in less than 1 ms. Other data sets showed similar or slower fluorescence onset, with the longest onset times being near 20 ms.

Fast mixing is crucial to the control and study of chemical reactions. In simple microfluidic devices, where flow is laminar, mixing is generally diffusion limited and dispersion of the reagents in the parabolic flow field is problematic. Turbulent flows solve these problems and provide very fast mixing but require very high pressure and flow rates and geometries that can be difficult to implement.⁴⁸ The use of droplets to confine the reagents in a flow field has many advantages, including the elimination of dispersion. Song et al.²⁰ used a simple geometric mixer to mix the contents of large “plug” droplets ($45 \mu\text{m}$ deep by $28 \mu\text{m}$ wide by variable length) in about 2 ms. Here the use of small droplets makes similar mixing times possible via diffusion.

To estimate the mixing time for droplets, multiple times scales must be considered. The droplets in this study coalesce spontaneously. The Triton X-100, which is soluble in the aqueous phase,

(48) Shastry, M. C. R.; Luck, S. D.; Roder, H. *Biophys. J.* **1998**, *74*, 2714–2721.

does not stabilize the droplets. The droplet coalescence time is therefore dominated by the effects of surface tension and viscous drag. In Figure 5, a small droplet with $r_s \approx 0.25 \mu\text{m}$ coalesces with a large droplet, $r_l \approx 1.5 \mu\text{m}$. The small droplet is fixed in the optical trap. After the droplets contact each other, the large droplet is pulled toward the small with a force given roughly by $2\sigma\pi r_s$, where $\sigma \approx 10 \text{ mN/m}$ is the surface tension of water and surfactant in FC-70.⁴⁹ Limited by the drag on the large droplet, the time for the large droplet to move one small droplet diameter is of the order $1 \mu\text{s}$, given that the dynamic viscosity of FC-70 is 1.3 cP . Diffusion is a slower process, and mixing time will therefore be diffusion dominated. The diffusion constant for CaCl_2 in aqueous solution is $1.1 \times 10^{-9} \text{ m}^2/\text{s}$ at room temperature,⁵⁰ which gives a diffusion time of $38 \mu\text{s}$ across the diameter of the small droplet. Meanwhile, Fluo-3 dye diffuses out of the small droplet volume into the larger coalesced volume. For Fluo-3 dye diffusing in buffer, the diffusion constant is⁵¹ $D \approx 0.8 \times 10^{-10} \text{ m}^2/\text{s}$ and the diffusion time across the large droplet radius is nearly 5 ms . The reaction rate for Fluo-3 and Ca^{2+} is expected to be diffusion limited.⁵² We therefore expect that the initial onset of fluorescence seen in Figure 5B corresponds primarily to the diffusion time of Ca^{2+} into the Fluo-3 containing region, and the longer decay time after the onset corresponds roughly to diffusion of Fluo-3 in the larger volume. Photobleaching also contributes to the decay of fluorescence. The presence of the optical tweezer and other hydrodynamic forces may also come into play and might account for the longer (10–20 ms) fluorescence onset times seen in some mixing data.

DISCUSSION

In single-molecule sensitive measurements, it is typical to confine a molecule to a detection region for purposes of background rejection and so that a single molecule can be observed over time. Common techniques for confinement such as surface binding,^{53–55} surface adsorption,^{56–59} or confinement in a porous material^{60,61} introduce inhomogeneities and can require chemical modification of the molecules under study. In contrast, the

chemical and physical environment afforded by droplets is far more homogeneous and reproducible, which minimizes artifacts and simplifies data analysis in single molecule measurement. The water/perfluorocarbon interface can be tailored with the addition of amphiphiles more easily than a glass surface can be modified. Fast mixing afforded by the subfemtoliter droplets makes these ideal bioreactors for studies of out-of-equilibrium dynamics and complex kinetics.

Like droplet confinement, liposome encapsulation^{65–67} solves the confinement problem and eliminates inhomogeneities related to the surface. In addition, liposome confinement enables the study of membrane proteins. Droplet confinement can be advantageous for the study of water-soluble molecules since the molecules do not partition into the continuous phase, obviating the need for a purification step. Droplet confinement is also useful when nano-container mixing is desired, since mixing liposomes requires disruption of the membrane, which can lead to loss of contents. Control of the chemical environment is generally simpler in droplets: droplets mix on contact and without loss of contents; photoactivation using a UV laser will not damage or destroy the droplet; and the application of other techniques, such as temperature jump,^{62–64} can be engineered to not perturb or disrupt the droplet.

Injected droplets present us with many new possibilities for the study of biomolecules. Many water-soluble proteins simply cannot be studied confined on a surface, since the surface adversely affects their function or even causes denaturation.⁶⁸ Droplets provide a simple and elegant solution for studying folding or remodeling of proteins that are inactive on surfaces. Droplets are also useful in the study of molecular complexes that are transiently interacting. Typically, single molecular complexes are observed tethered to surfaces, but only long-lived complexes such as highly processive enzymes on DNA are easily studied this way. Within the small volume of a 1 fL droplet, individual molecules can have effective concentrations higher than 1 nmol/L , with a corresponding diffusion-limited collision rate for two moderately sized molecules ($D = 4 \times 10^{-11} \text{ m}^2/\text{s}$, molecular mass $\approx 50 \text{ kDa}$) of several thousand interactions per second.⁶⁹ Droplets can therefore be used to confine and study the components of a single transient complex. Finally, multiple injectors can be used to introduce different molecular species on demand. With optical or fluidic techniques for droplet manipulation and coalescence, droplet reactors might ultimately be used for the bottom-up assembly of individual biomolecular complexes.

- (49) Li, L.; Mustafi, D.; Fu, Q.; Tereshko, V.; Chen, D. L. L.; Tice, J. D.; Ismagilov, R. F. *Proc. Natl. Acad. Sci. U.S.A.* **2006**, *103*, 19243–19248.
- (50) Ribeiro, A. C. F.; Barros, M. C. F.; Teles, A. S. N.; Valente, A. J. M.; Lobo, V. M. M.; Sobral, A. J. F. N.; Esteso, M. A. *Electrochim. Acta* **2008**, *54*, 192–196.
- (51) Brown, E. B.; Shear, J. B.; Adams, S. R.; Tsien, R. Y.; Webb, W. W. *Biophys. J.* **1999**, *76*, 489–499.
- (52) Eberhard, M.; Erne, P. *Biochem. Biophys. Res. Commun.* **1989**, *163*, 309–314.
- (53) Ha, T.; Zhuang, X. W.; Kim, H. D.; Orr, J. W.; Williamson, J. R.; Chu, S. *Proc. Natl. Acad. Sci. U.S.A.* **1999**, *96*, 9077–9082.
- (54) Noji, H.; Yasuda, R.; Yoshida, M.; Kinosita, K. *Nature* **1997**, *386*, 299–302.
- (55) Wennmalm, S.; Edman, L.; Rigler, R. *Proc. Natl. Acad. Sci. U.S.A.* **1997**, *94*, 10641–10646.
- (56) Bopp, M. A.; Jia, Y. W.; Li, L. Q.; Cogdell, R. J.; Hochstrasser, R. M. *Proc. Natl. Acad. Sci. U.S.A.* **1997**, *94*, 10630–10635.
- (57) Jia, Y. W.; Talaga, D. S.; Lau, W. L.; Lu, H. S. M.; DeGrado, W. F.; Hochstrasser, R. M. *Chem. Phys.* **1999**, *247*, 69–83.
- (58) Talaga, D. S.; Lau, W. L.; Roder, H.; Tang, J. Y.; Jia, Y. W.; DeGrado, W. F.; Hochstrasser, R. M. *Proc. Natl. Acad. Sci. U.S.A.* **2000**, *97*, 13021–13026.
- (59) Wazawa, T.; Ishii, Y.; Funatsu, T.; Yanagida, T. *Biophys. J.* **2000**, *78*, 1561–1569.
- (60) Dickson, R. M.; Cubitt, A. B.; Tsien, R. Y.; Moerner, W. E. *Nature* **1997**, *388*, 355–358.
- (61) Lu, H. P.; Xun, L. Y.; Xie, X. S. *Science* **1998**, *282*, 1877–1882.

- (62) Xu, Y.; Wang, T.; Gai, F. *Chem. Phys.* **2006**, *323*, 21–27.
- (63) Eaton, W. A.; Munoz, V.; Hagen, S. J.; Jas, G. S.; Lapidus, L. J.; Henry, E. R.; Hofrichter, J. *Annu. Rev. Biophys. Biomol. Struct.* **2000**, *29*, 327–359.
- (64) Phillips, C. M.; Mizutani, Y.; Hochstrasser, R. M. *Proc. Natl. Acad. Sci. U.S.A.* **1995**, *92*, 7292–7296.
- (65) Boukobza, E.; Sonnenfeld, A.; Haran, G. *J. Phys. Chem. B* **2001**, *105*, 12165–12170.
- (66) Okumus, B.; Wilson, T. J.; Lilley, D. M. J.; Ha, T. *Biophys. J.* **2004**, *87*, 2798–2806.
- (67) Yoon, T. Y.; Okumus, B.; Zhang, F.; Shin, Y. K.; Ha, T. *Proc. Natl. Acad. Sci. U.S.A.* **2006**, *103*, 19731–19736.
- (68) Friedel, M.; Baumketner, A.; Shea, J. E. *J. Chem. Phys.* **2007**, *126*.
- (69) Chiu, D. T.; Wilson, C. F.; Karlsson, A.; Danielsson, A.; Lundqvist, A.; Stromberg, A.; Ryttsen, F.; Davidson, M.; Nordholm, S.; Orwar, O.; Zare, R. N. *Chem. Phys.* **1999**, *247*, 133–139.

ACKNOWLEDGMENT

We thank Dr. John J. Kasianowicz for the use of the Sutter P-2000 micropipet puller, Dr. Kimberly A. Briggman for advice on hydrophobic coating, and 3M Corp. for providing FC-70 fluorocarbon. We also thank Drs. Jeeseong Hwang, John Woodward, Alice Crawford, Christian Santangelo, and Anthony Dinsmore for helpful discussion. This work was supported by NIST, the Office of Naval Research, and NSF Grant MCB-0920139. Certain commercial equipment, instruments, or materials are identified in this paper to foster understanding. Such identification does not imply recommendation or endorsement

by the National Institute of Standards and Technology nor does it imply that the materials or equipment identified are necessarily the best available for the purpose.

SUPPORTING INFORMATION AVAILABLE

Additional information as noted in text. This material is available free of charge via the Internet at <http://pubs.acs.org>.

Received for review June 30, 2009. Accepted August 12, 2009.

AC9014319